

Comparative Analysis of TCAD augmented ML Algorithms in modeling of AlGa_N/Ga_N HEMTs

Shivansh Awasthi
Centre for Applied Research in Electronics
Indian Institute of Technology
Delhi, India
shivanshawasthi27@gmail.com

Vikas Kumar
Centre for Applied Research in Electronics
Indian Institute of Technology
Delhi, India
crz218466@iitd.ac.in

Pragyey Kumar Kaushik
Centre for Applied Research in Electronics
Indian Institute of Technology
Delhi, India
pragyeykumarkausik@gmail.com

Ankur Gupta
Centre for Applied Research in Electronics
Indian Institute of Technology
Delhi, India
ankur.care.iitd@gmail.com

Abstract— In this study, a computer-aided design (TCAD) supported machine learning framework is built to predict the intrinsic parameters of Ga_N HEMT, such as V_{TH} (Threshold Voltage) and g_m (Transconductance). TCAD was used to generate the training data set constituting the I_D - V_{GS} characteristics of the Ga_N HEMT. This is achieved by changing multiple input parameters (e.g. the Al mole fraction (x), gate metal work function, AlGa_N barrier thickness and gate length). We deployed numerous ML algorithms and an ANN (artificial neural network) to predict the V_{TH} and g_m of Ga_N HEMT. We compared the performance of these ML algorithms and found that the boosting and ensemble algorithms provide better results in terms of accuracy. We showed that Random Forest and Gradient Boost were most effective in predicting V_{TH} with an R^2 value of 0.99 each, and for g_m prediction, Gradient Boost was most effective with an R^2 of 0.92.

Keywords— *ann, gan hemt, gradient boost, machine learning, tcad, threshold voltage, transconductance*

I. INTRODUCTION

Ga_N HEMTs (Gallium nitride-based high electron mobility transistors) are a desirable and promising candidate for high power and high-frequency electronic applications owing to their distinct material properties such as a wide band gap (3.4 eV) and high saturation velocity (2.5×10^7 cm/s) [1], [2]. Owing to these properties, Ga_N HEMTs are used for space applications [3], RADARs [4], mixers [5], THz detectors [6] and high-speed RF circuits [7]. TCAD-integrated (ML) machine learning and (DL) deep learning have gained increasing popularity in the past few years due to the availability of highly efficient computational systems [8]–[10]. Machine learning and deep learning require a large amount of data for training the models, which acts as a barrier to their usage across various industries, such as microelectronics [11]. Data generation for these HEMT devices is very cumbersome because the characterization of devices is costly and time-consuming. Therefore, it is more efficient to use TCAD for generating data by varying device structure, process, and material parameters. It is also used to establish a relationship between input and output which can further be utilized for the prediction of significant device parameters, which is otherwise a tedious process owing to the heterostructure of HEMTs and their complex device physics [12].

TCAD-augmented ML and artificial neural networks have already been used in the past to model junction-less nanowires [13], [10], and other devices [8]. However, these reported methods suffer from outliers or weak learners, leading to models not being applicable to non-linear data. Regression algorithms [14], [15] have been used in the past to predict HEMT's parameters; however, they produce inaccurate results when the relationship in the data is non-linear, non-monotonic and complex [8]–[10].

In this work, we encountered these issues using (GB) Gradient Boost [16] and (RF) Random Forest algorithms [17]. We compared the performance of different ML algorithms and determined which ML algorithm was accurate and robust for the prediction of V_{TH} and g_m of Ga_N HEMT. For the first time, we use a Gradient Boosting algorithm to predict the intrinsic parameters of Ga_N HEMT.

II. DEVICE DESIGN, SIMULATION SETUP AND DATA SET PREPARATIONS

The 2D structure of the AlGa_N/Ga_N HEMT used in this study is illustrated in Fig. 1 (a). It has a barrier layer (t_{AlGaN}) of 30 nm, and the thickness of the Ga_N buffer (t_{GaN}) used is 2 μ m. The drain to source spacing and gate to drain spacing is 2.5 μ m, respectively. The length of the gate was 1 μ m, and the width of the device was 150 μ m. The transfer characteristics of the device are shown in Fig. 1 (b) [18]. The calibration [18] was done using the Sentaurus TCAD version 2018.06-SPI [19].

The TCAD Lombardi model and Philip unified mobility models are used to account for the carrier, impurity scattering and mobility degradation at the interfaces. The SRH (Shockley Read Hall) and Auger models are used for recombination properties through deep defect levels and traps. The drift-diffusion model [20] was used to set up the transport properties of carriers along with the Fermi statistics. The intrinsic device parameters investigated and varied were Al mole fraction (x), gate length (L_G), barrier thickness (T_B), and gate metal work function (WF), as shown in Table I. Fig. 2 shows a subset of the training data set used to train the machine learning model. Several Transfer characteristics (I_D - V_G) and transconductance curves g_m of the Ga_N HEMT are simulated with the variation of the input parameters mentioned in Table I.

III. ML ALGORITHMS AND IMPLEMENTATION STRATEGY

The TCAD data generated for multiple parameters, as described in the previous section, are used in the implementation of machine learning algorithms for prediction and modelling purposes. The process flow and strategy for implementation are shown in Fig.3. Data preprocessing [21] involves importing all the libraries and cleaning the data. The data was standardized according to the z score [22] with a mean value of 0 and a standard deviation of 1, as shown in (1).

$$z = \frac{(x - \mu)}{\sigma} \quad (1)$$

After defining the input features and output labels, the Scikit learn library [23] was used to implement the machine learning algorithms. Then, the pandas data frame [24] was used for splitting the data set into training and test set. Seventy percent of the data was allotted for training and building the models, whereas thirty percent of the data was used for evaluating the test set. Subsequently, the models were evaluated according to the coefficient of determination.

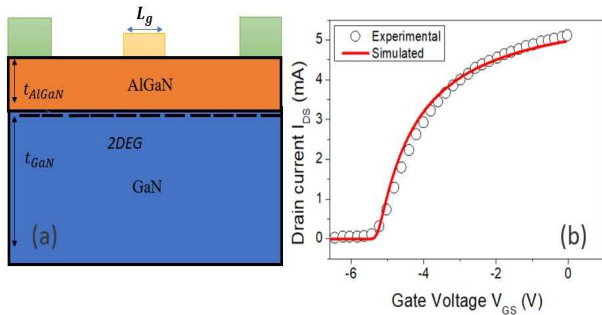


Fig. 1. a. 2D device structure of GaN HEMT used for simulation b. Simulated Transfer characteristics calibrated with experimental data [18].

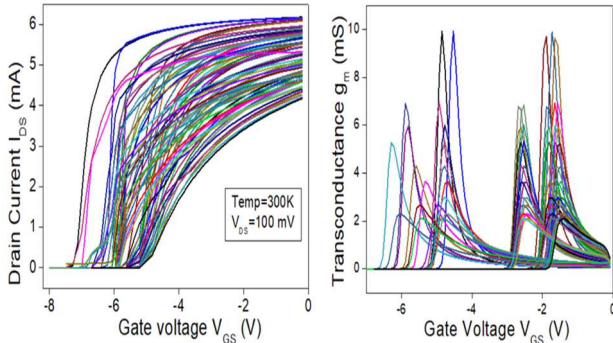


Fig. 2. Subset of Training Data a. Transfer Characteristics and b. Transconductance of GaN HEMT used for training of ML and ANN by variation of parameters in Table I.

Table I The list of parameters varied to create ML data set

Parameter	Value
Al mole fraction (x)	0.15 to 0.3
AlGaIn Barrier Thickness (t_{AlGaIn})	18 nm to 30 nm
Work Function (WF)	4.1 eV to 6.1 eV
Gate Length	100 nm to 1.8 μ m

The ML algorithms used in this work for the prediction of threshold voltage and transconductance of GaN HEMT are Ridge and Lasso Regression [25], [26], Random Forest, and Gradient Boost.

IV. RESULTS AND DISCUSSION

In this study, the first ridge and LASSO regression were used to predict the value of V_{TH} and g_m by varying four input parameters (Al mole fraction, AlGaIn barrier thickness and gate length, and gate metal work function). Fig. 4 shows the scatter plot of the predicted and actual values of the threshold voltage and transconductance, along with the coefficient of determination R^2 [27]. Lasso regression gives an R^2 value of 0.96 for V_{TH} prediction and 0.74 for g_m , as shown in Fig.4 (c) & 4(d). Ridge Regression gives R^2 value of 0.95 for V_{TH} and 0.73 for g_m , as shown in Fig. 4 (a) and 4 (b). K-fold cross-validation was used to evaluate model accuracy after tuning the model's hyperparameters. Ridge regression provides an

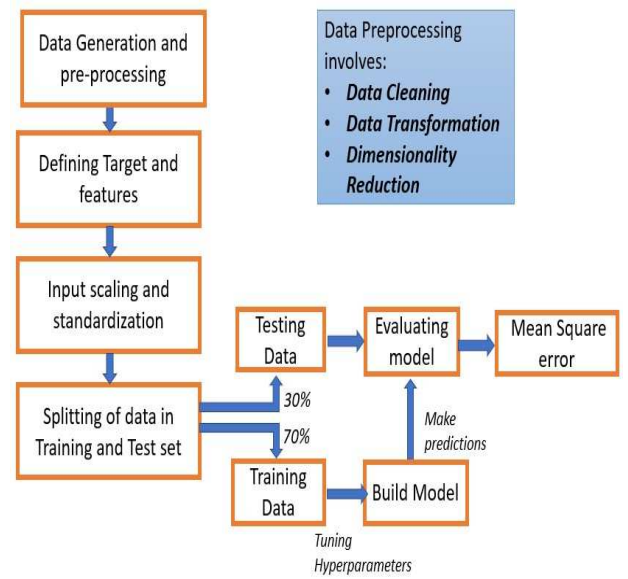


Fig. 3. Process flow diagram of Machine learning model development, prediction, and validation.

optimized mathematical equation (2) that is useful for the prediction of V_{TH} . The mathematical equation and their respective coefficients are given in (2) and Fig. 5, respectively.

$$V_{TH} = A(\text{Al mole fraction}) + B(\text{Gate Metal Work function}) + C(\text{AlGaIn Barrier Thickness}) + D(\text{Gate Length}) + \text{constant} \quad (2)$$

The negative value of the coefficient (mole fraction and barrier thickness) indicates that if we increase their values, the threshold voltage will decrease and vice versa. This shows that with the decrease in mole fraction and barrier thickness, the 2DEG charge is reduced; hence, the threshold voltage is increased. An increase in work function will also increase the threshold voltage as it increases the barrier height and lifts the conduction band. This leads to fewer charges in 2DEG. [28], [29]. However, ridge and lasso regression, as shown in Fig 4a-4c, were helpful in predicting V_{TH} . However, a lesser value of R^2 in the case of g_m shows that these algorithms fail in the prediction when there is a non-linear, complex and non-monotonic relationship in the data. The drawback of overfitting and high bias in the regression models discussed above were solved by Random Forest and Gradient Boost

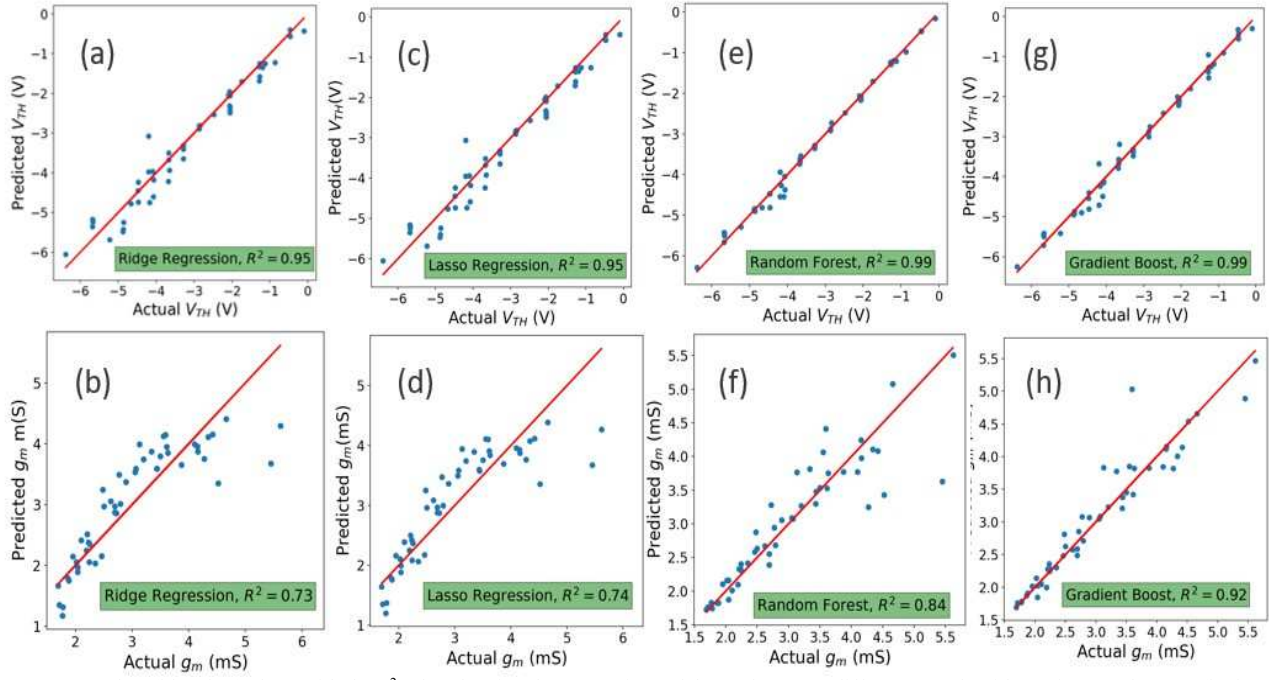


Fig. 4. Scatter plots (blue dots) along with the R^2 value showing the comparison of the performance different ML algorithm using test data. (a)-(b) for Ridge Regression, (c)-(d) for Lasso Regression, (e)-(f) for Random Forest and (g)-(h) for Gradient Boost.

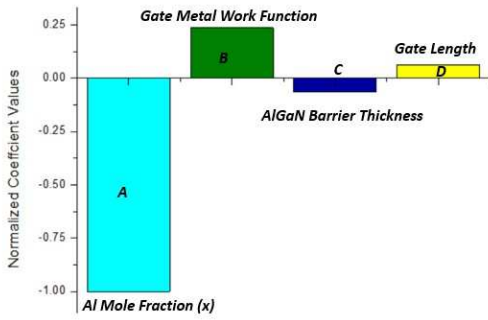


Fig. 5. Normalized Coefficients in the equation of threshold voltage developed by Ridge Regression ML algorithm.

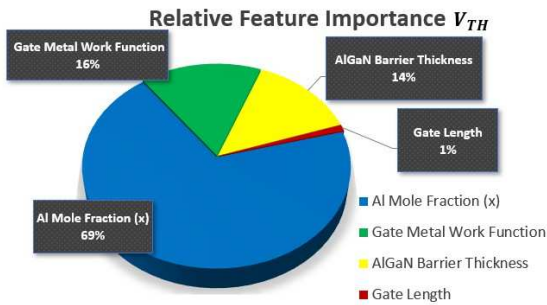


Fig. 6 Relative weight of each feature in modeling Threshold Voltage given by Random Forest ML algorithm.

algorithms. The R^2 value for the Random Forest for V_{TH} and g_m is 0.99 and 0.84, respectively, as seen in Fig. 4e and Fig. 4f, respectively. The predictions are more accurate and stable when compared to the ridge and lasso regression. This is further improved significantly by the use of ensemble and boosting algorithms, such as the Gradient Boost algorithm, which gives an R^2 value of 0.99 for V_{TH} and 0.92 for g_m , as seen in Fig. 4g and Fig. 4h, respectively. This improvement is due to the fact that the Gradient Boost algorithm takes into account the non-monotonic relationship between the

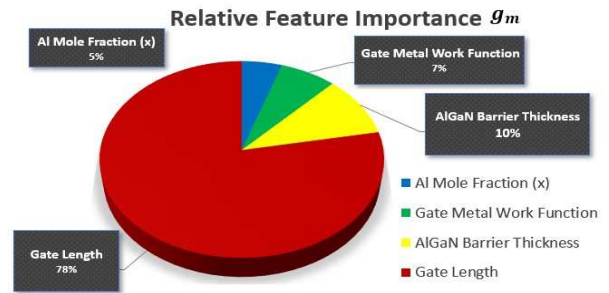


Fig. 7. Relative weight of each feature in modeling transconductance given by Random Forest ML algorithm.

variables more accurately. The weights from the random forest are shown in Fig. 6 and Fig. 7 for V_{TH} and g_m respectively. The R^2 value between 0.84 to 0.99 signifies that the device physics has been captured accurately. We also developed for comparison a multi-layer Deep Artificial Neural Network is also developed for the modelling of the V_{TH} and g_m containing an input layer with four nodes and four hidden layers with 64, 32, 16 and 8 nodes, respectively, not shown in this work. The activation function used in the development of this ANN is the RELU [30] function, and Adam optimization [31] is used for 150 epochs.

All the results from ML model were further validated with calibrated TCAD simulations. From Fig. 8a. and Fig. 8b, it is evident that Ridge Regression is less accurate for the prediction of V_{TH} and especially g_m , as there is a significant mismatch between the simulated and model results. The match for models of Random Forest, Gradient Boost and ANN in prediction is shown in Fig. 8(c)-(h). It can be seen that the use of Random Forest and Gradient Boost algorithm proved to be more accurate for predictions. They also have a better match, as shown in Fig 8(c)-8(h). The relative improvement in the case of g_m shows how regression and regularization algorithms fail to predict when there is a non-linear relationship between input and output. A comparison

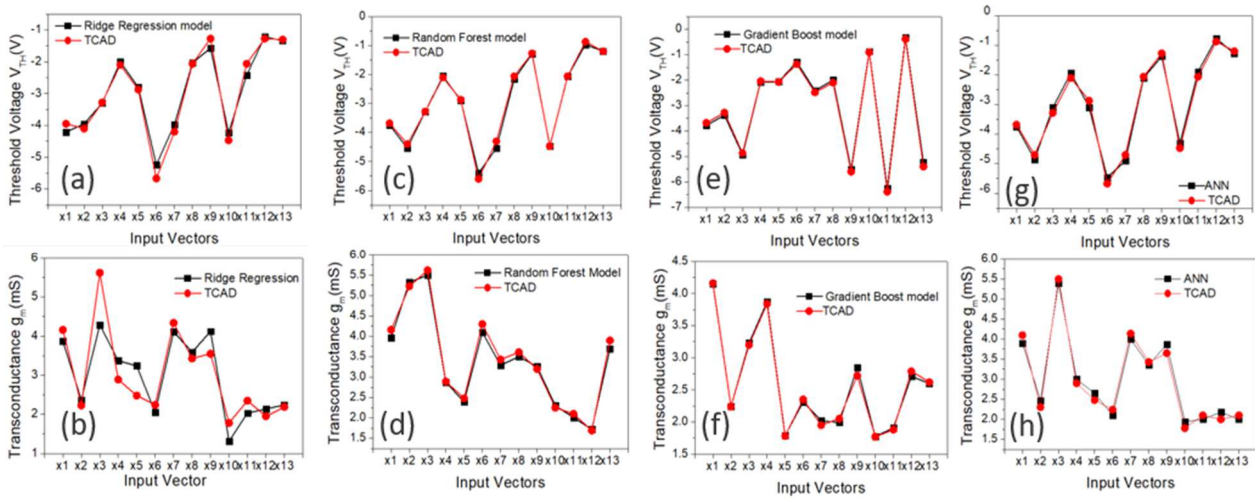


Fig. 8. Comparison of model results and TCAD results for (a) and (b) Ridge regression, (c) and (d) Random Forest, (e) and (f) Gradient Boost, (g) and (h) ANN.

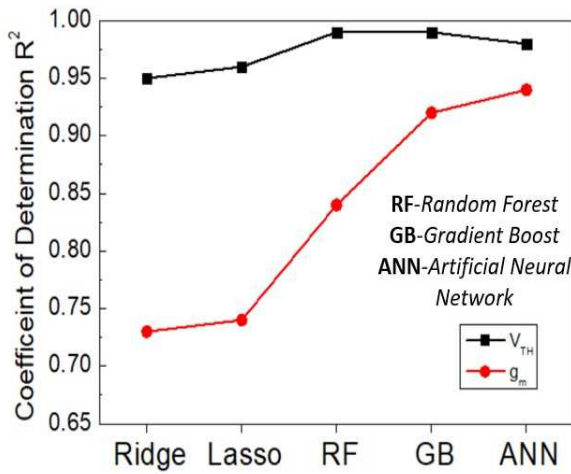


Fig. 9. Comparison of the different ML algorithms and ANN in the prediction of V_{TH} (black dots) and g_m (red dots), respectively.

of all the algorithms related to their prediction of V_{TH} and g_m was performed using the coefficient of determination, as shown in Fig. 9. The better results of Random Forest are due to the fact that it averages out results from all the trees and provides the output. The Gradient Boost algorithm ensures boosting the performance of weak learners among the data and hence improving results. These ensemble and boosting algorithms provide performance at par with ANN, which is a good thing as implementation requires ANN to have more GPU power, is slower and requires more data. [32]

V. CONCLUSION

Ensemble and boost algorithms (i.e., Gradient Boost algorithm) and Random Forest algorithm are used to predict V_{TH} and g_m based on structural and material parameters. Ridge and Lasso regression were also implemented to develop a mathematical equation that helps in modelling V_{TH} . It was found that regression algorithms were not efficient in the prediction of g_m with an R^2 value of 0.73. Hence, the Random Forest and Gradient Boost ML algorithms, which are a collection of decision tree models, were implemented, which improved the prediction of g_m with an R^2 value of 0.84 and 0.92, respectively. Furthermore, the performance of the Gradient Boost algorithm was found to be at par with that of ANN.

ACKNOWLEDGEMENT

This work was supported by the Defence Research and Development Organization (DRDO) Govt. of India under Grant JATC-EMDTERA-06.

REFERENCES

- [1] U. K. Mishra, P. Parikh, and Y.-F. Wu, "Algan/gan hemts-an overview of device operation and applications," *Proceedings of the IEEE*, vol. 90, no. 6, pp. 1022–1031, 2002.
- [2] U. K. Mishra, Y.-F. Wu, B. P. Keller, S. Keller, and S. P. Denbaars, "Gan microwave electronics," *IEEE transactions on microwave theory and techniques*, vol. 46, no. 6, pp. 756–761, 1998.
- [3] E. Suijker, M. Rodenburg, J. Hoogland, M. Van Heijningen, M. Seelmann-Eggebert, R. Quay, P. Bruckner, and F. E. van Vliet, "Robust algan/gan low noise amplifier mmics for c-, ku-and ka-band space applications," in *2009 Annual IEEE Compound Semiconductor Integrated Circuit Symposium*. IEEE, 2009, pp. 1–4.
- [4] R. S. Pengelly, S. M. Wood, J. W. Milligan, S. T. Sheppard, and W. L. Pribble, "A review of gan on sic high electron-mobility power transistors and mmics," *IEEE Transactions on Microwave Theory and Techniques*, vol. 60, no. 6, pp. 1764–1783, 2012.
- [5] M. Sudow, K. Andersson, M. Fagerlind, M. Thorsell, P.-A. Nilsson, and N. Rorsman, "A single-ended resistive x-band algan/gan hemt mmic mixer," *IEEE transactions on Microwave Theory and Techniques*, vol. 56, no. 10, pp. 2201–2206, 2008.
- [6] M. Bauer, A. Ramer, S. A. Chevtchenko, K. Y. Osipov, D. Cibiraitė, S. Pralgauskaitė, K. Ikamas, A. Lisauskas, W. Heinrich, V. Krozer et al., "A high-sensitivity algan/gan hemt terahertz detector with integrated broadband bow-tie antenna," *IEEE Transactions on Terahertz Science and Technology*, vol. 9, no. 4, pp. 430–444, 2019.
- [7] T. Kazior, R. Chelakara, W. Hoke, J. Bettencourt, T. Palacios, and H. Lee, "High performance mixed signal and rf circuits enabled by the direct monolithic heterogeneous integration of gan hemts and si cmos on a silicon substrate," in *2011 IEEE Compound Semiconductor Integrated Circuit Symposium (CSICS)*. IEEE, 2011, pp. 1–4.
- [8] H. Dhillon, K. Mehta, M. Xiao, B. Wang, Y. Zhang, and H. Y. Wong, "Tcad-augmented machine learning with and without domain expertise," *IEEE Transactions on Electron Devices*, vol. 68, no. 11, pp. 5498–5503, 2021.
- [9] K. Mehta and H.-Y. Wong, "Prediction of finfet current-voltage and capacitance-voltage curves using machine learning with autoencoder," *IEEE Electron Device Letters*, vol. 42, no. 2, pp. 136–139, 2020.
- [10] T.-L. Wu and S. B. Kutub, "Machine learning-based statistical approach to analyze process dependencies on threshold voltage in recessed gate algan/gan mis-hemts," *IEEE Transactions on Electron Devices*, vol. 67, no. 12, pp. 5448–5453, 2020.
- [11] S. Butte, A. Prashanth, and S. Patil, "Machine learning based predictive maintenance strategy: a super learning approach with deep neural networks," in *2018 IEEE Workshop on Microelectronics and Electron Devices (WMED)*. IEEE, 2018, pp. 1–5.

- [12] S. A. Vitusevich, A. M. Kurakin, N. Klein, M. V. Petrychuk, A. V. Naumov, and A. E. Belyaev, "Algan/gan high electron mobility transistor structures: self-heating effect and performance degradation," *IEEE transactions on device and materials reliability*, vol. 8, no. 3, pp. 543–548, 2008.
- [13] H. Carrillo-Nunez, N. Dimitrova, A. Asenov, and V. Georgiev, "Machine learning approach for predicting the effect of statistical variability in si junctionless nanowire transistors," *IEEE Electron Device Letters*, vol. 40, no. 9, pp. 1366–1369, 2019.
- [14] Y. Ren, L. Zhang, and P. N. Suganthan, "Ensemble classification and regression-recent developments, applications and future directions," *IEEE Computational intelligence magazine*, vol. 11, no. 1, pp. 41–53, 2016.
- [15] R. Muthukrishnan and R. Rohini, "Lasso: A feature selection technique in predictive modeling for machine learning," in *2016 IEEE international conference on advances in computer applications (ICACA)*. IEEE, 2016, pp. 18–20.
- [16] P. Prettenhofer and G. Louppe, "Gradient Boosted regression trees in scikit-learn," 2014.
- [17] A. Paul, D. P. Mukherjee, P. Das, A. Gangopadhyay, A. R. Chintha, and S. Kundu, "Improved Random Forest for classification," *IEEE Transactions on Image Processing*, vol. 27, no. 8, pp. 4012–4024, 2018.
- [18] D. Pradeep, M. Amit, and S. Karmalkar, "Dc extraction of gate biasdependent parasitic resistances and channel mobility in an hemt," *IEEE Electron Device Letters*, vol. 37, no. 11, pp. 1403–1406, 2016.
- [19] T. Sentaurus, "O-2018.06 manual," Mountain View, CA, USA, Synopsys, 2018.
- [20] V. Joshi, A. Soni, S. P. Tiwari, and M. Shrivastava, "A comprehensive computational modeling approach for algan/gan hems," *IEEE Transactions on Nanotechnology*, vol. 15, no. 6, pp. 947–955, 2016.
- [21] L. Zheng, W. Hu, and Y. Min, "Raw wind data preprocessing: A datamining approach," *IEEE Transactions on Sustainable Energy*, vol. 6, no. 1, pp. 11–19, 2014.
- [22] A. E. Curtis, T. A. Smith, B. A. Ziganshin, and J. A. Elefteriades, "The mystery of the z-score," *Aorta*, vol. 4, no. 04, pp. 124–130, 2016.
- [23] P. Gijsbers, E. LeDell, J. Thomas, S. Poirier, B. Bischl, and J. Vanschoren, "An open source automl benchmark," *arXiv preprint arXiv:1907.00909*, 2019.
- [24] W. McKinney *et al.*, "pandas: a foundational python library for data analysis and statistics," *Python for high performance and scientific computing*, vol. 14, no. 9, pp. 1–9, 2011.
- [25] W. Chiang, X. Liu, T. Zhang, and B. Yang, "A study of exact ridge regression for big data," in *2018 IEEE International Conference on Big Data (Big Data)*. IEEE, 2018, pp. 3821–3830.
- [26] J. Ottaway, J. H. Kalivas, and E. Andries, "Spectral multivariate calibration with wavelength selection using variants of tikhonov regularization," *Applied spectroscopy*, vol. 64, no. 12, pp. 1388–1395, 2010.
- [27] Y. Dodge, "Coefficient of determination," *The Concise Encyclopedia of Statistics*, pp. 88–91, 2008.
- [28] A. Malik, N. Jain, M. Mishra, S. Kumar, D. Rawal, A. Singh *et al.*, "Analytical model to evaluate threshold voltage of gan based hemt involving nanoscale material parameters," *Superlattices and Microstructures*, vol. 152, p. 106834, 2021.
- [29] A. Malik, P. Kamboj, S. Awasthi, P. Thakur, N. Jain, M. Mishra, S. Kumar, D. S. Rawal, A. K. Singh *et al.*, "Parameter-based modeling of nanoscale material thermal noise in gallium nitride high-electronmobility transistors," *Semiconductor Science and Technology*, vol. 36, no. 3, p. 035004, 2021.
- [30] A. F. Agarap, "Deep learning using rectified linear units (relu)," *arXiv preprint arXiv:1803.08375*, 2018.
- [31] I. K. M. Jais, A. R. Ismail, and S. Q. Nisa, "Adam optimization algorithm for wide and deep neural network," *Knowledge Engineering and Data Science*, vol. 2, no. 1, pp. 41–46, 2019.
- [32] A. Wolfewickz "Deep Learning vs. Machine Learning – What's The Difference?" <https://levity.ai/blog/difference-machine-learning-deep-learning> (Accessed: September, 29 2022)